water

MDPI

Article

Industry-Driven Versus Natural Groundwater Flow Regime at the Dead Sea Coastal Aquifer

Yehuda Levy [1,2,*] and Haim Gvirtzman [1]

[1] Institute of Earth Sciences, The Hebrew University, Jerusalem 91904, Israel; haim.gvirtzman@mail.huji.ac.il
[2] Department of Earth and Planetary Sciences, Weizmann Institute of Science, Rehovot 7610001, Israel.
* Correspondence: yehuda.levy1@mail.huji.ac.il

Supplementary Materials

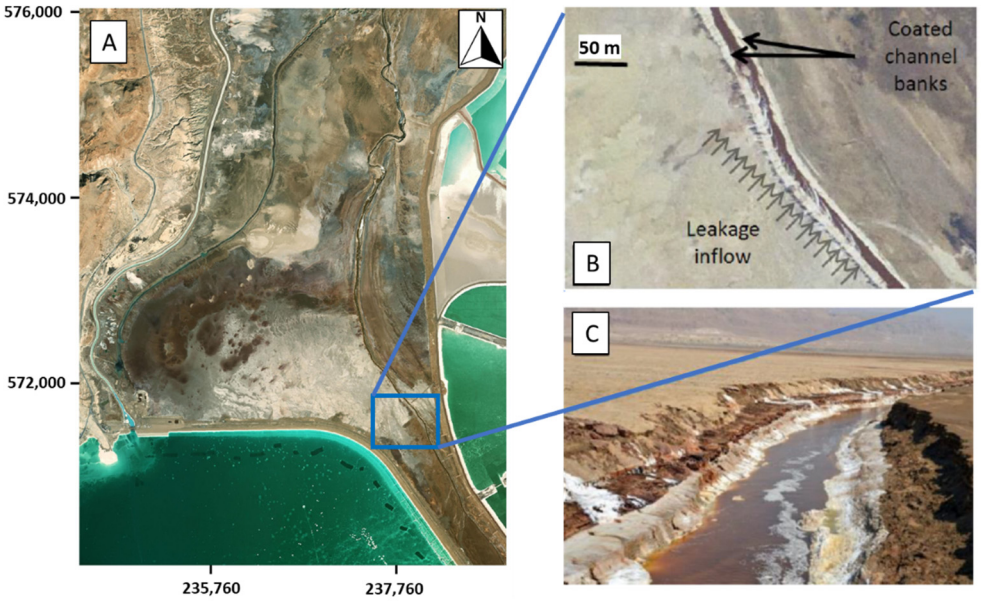

Figure S1. Halite precipitation above the stream bank, between the northeastern corner of the evaporation ponds and the Arava stream, resulting from brine leakage. (**A**) Location map. (**B**) Enlargement of the leaking area. (**C**) Patches of salt precipitation along the stream bank (after Dente et al., 2017).

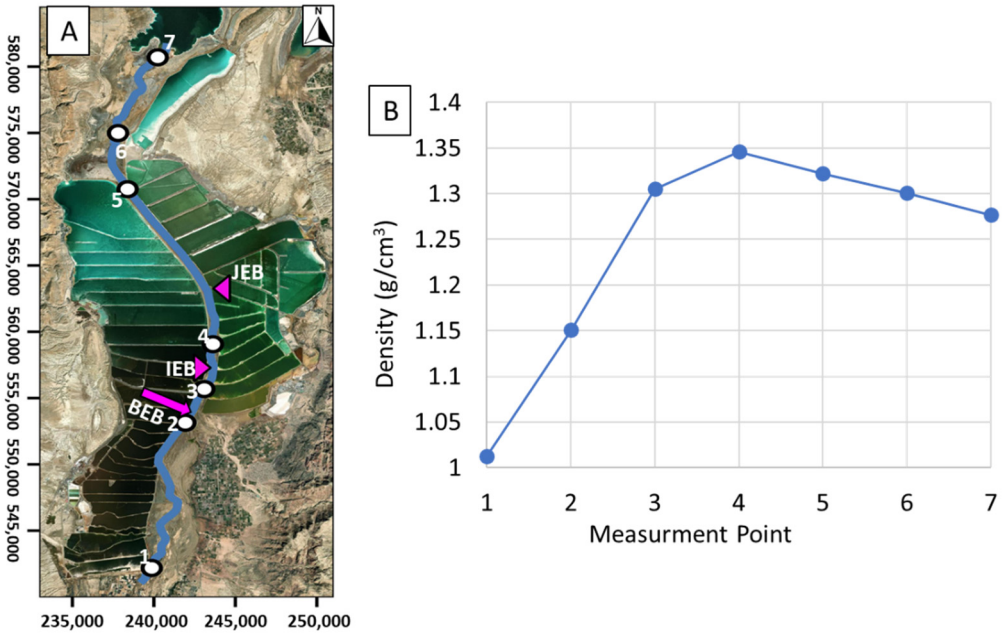

Figure S2. Evidence of brine leakage along the Arava stream based on changes in water density (based on Sheffer, 2013 [24]). (**A**) Map of the sampling points, marked 1 to 7 from south to north. (**B**) Measured water densities show an increase between points 1 and 4 due to the entrance of end brines from the bromine factory (BEB) and from the Israeli (IEB) and Jordanian (JEB) potash factories, and a decrease between points 4 and 7 due to leakage from the evaporation ponds.

Figure S3. (**A**) Measuring water discharge in the marine canal at several points throughout the flow section. (**B**) Using a propeller-type current meter.

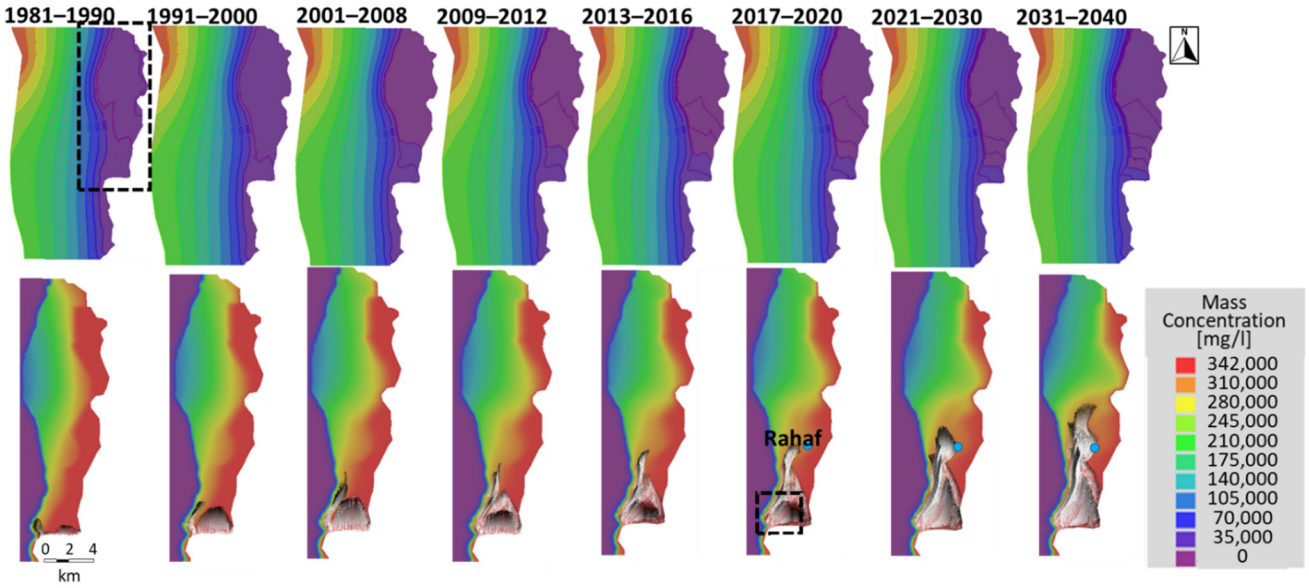

Figure S4. Maps of groundwater level (meters above sea level, top row) and salinity distributions (bottom row) for each of the time steps (past reconstruction and future predictions). The head contour difference is 50 m in general but 10 m between the ponds and the lake, where the increasing gradient with time is notable. Note the brine washing with time on the newly exposed land. The black–white lines are particle tracking of brine leakage from the pond's northern embankment progressing toward Rahaf borehole. The dashed rectangular area on the left top map represents the enlarged area in the bottom row maps. The dashed rectangular area on the 2017–2020 period map (bottom row) is the area shown in Figure 11 in the main text.

Table S1. Geochemical parameters of the brines at several measurement points (based on Farber, 2016 [30]). The similarity between the first four values and the difference between these and the last two values indicate leakage from the evaporation ponds.

	Na/Cl	Mg/Cl	Ca/Mg	Ca/Cl	K/Cl	SO4/Cl	Br/Cl
Marine canal – north	0.1801	0.3112	0.273	0.0849	0.0317	0.00032	0.0076
Marine canal – south	0.1607	0.3147	0.2403	0.0756	0.0318	0.00029	0.0074
Feeding canal	0.1902	0.3062	0.2613	0.08	0.032	0.00037	0.0074
Halite pond - north	0.1755	0.3208	0.2378	0.0763	0.0323	0.00036	0.0077
Fresh groundwater (Ye'elim 4 borehole)	0.3585	0.2516	0.2906	0.0731	0.0245	0.0197	
Fresh groundwater (Ye'elim 2 borehole)	0.2345	0.2949	0.268	0.079	0.0297	0.00347	

Table S2. Mass balance calculations at the northern evaporation ponds for 2003–2018.

	Inflow					**Precipi-tation**	**Evaporation**			**Outflow**			**Leakage**		
Year	P88 in (mcm)	P88 den-sity (ton/m^3)	P88 in (Mton)	Rain (m)	Rain (mcm or Mton)	Halite perc. (Mton)	Evap (m)	Area (km^2)	Evap (mcm or Mton)	P11/33 out* (mcm)	P11/33 density (ton/m^3)	P11/33 out (Mton)	Leakage (Mton)	Leakage density (ton/m3)	Leak-age (mcm)
2003	363	1.23	448	0.025	2.2	21.3	1.32	88.9	117.4	193	1.29	249	63	1.26	**50**
2004	348	1.24	430	0.034	3.0	22.7	1.35	88.9	120.1	179	1.29	231	59	1.26	**47**
2005	385	1.24	477	0.026	2.3	24.3	1.28	88.9	113.8	206	1.29	266	76	1.26	**60**
2006	378	1.24	468	0.031	2.8	23.9	1.33	88.9	118.3	223	1.29	288	41	1.26	**32**
2007	353	1.24	438	0.029	2.4	21.0	1.34	81.9	109.8	192	1.29	247	63	1.27	**50**
2008	389	1.24	483	0.043	3.5	22.2	1.28	81.5	104.4	207	1.29	266	93	1.26	**74**
2009	406	1.24	504	0.011	0.9	23.3	1.27	83.1	105.6	203	1.29	262	114	1.27	**90**
2010	409	1.24	508	0.021	1.8	22.2	1.27	83.1	105.6	204	1.29	264	118	1.27	**93**
2011	448	1.24	557	0.034	2.8	22.6	1.24	83.1	103.1	205	1.29	265	169	1.27	**133**
2012	460	1.24	572	0.018	1.5	22.5	1.28	83.1	106.4	213	1.29	275	170	1.27	**134**
2013	407	1.24	506	0.034	2.8	23.5	1.25	83.1	103.9	233	1.29	300	81	1.27	**64**
2014	377	1.24	469	0.078	6.5	18.5	1.21	83.1	100.6	197	1.29	255	102	1.27	**80**
2015	375	1.25	467	0.084	7.0	19.5	1.25	83.6	104.5	209	1.29	270	80	1.27	**63**
2016	418	1.25	520	0.028	2.3	22.9	1.28	83.6	107.0	253	1.29	327	66	1.27	**52**
2017	422	1.25	525	0.024	2.0	22.4	1.28	83.6	107.0	232	1.29	301	97	1.27	**77**
2018	432	1.25	538	0.055	4.6	21.0	1.25	83.6	104.5	216	1.29	280	137	1.27	**108**

* Net pumping volumes at P11/P33, offsetting the plant return flows.

Table S3. Representative leakage volumes from the evaporation ponds for the different time periods (in accordance with Figure 6 in the main text).

Δt	**Years**	**Leakage (mcm/yr)**
1	1981–1990	20
2	1991–2000	35
3	2001–2008	50
4	2009–2012	110
5	2013–2016	60
6	2017–2020	80

Table S4. Constant head boundary conditions and total representative leakage volume for the different time periods, serving as input for the numerical modeling (in accordance with Figure 8 in the main text).

Δt	Years	Δh Arava (m)	Dead Sea level (m)	Pond level (m)	Leakage (mcm/yr)
1	1981–1990	3	-402	-394	20
2	1991–2000	5	-410	-393	35
3	2001–2008	7	-418	-392	50
4	2009–2012	9.5	-422	-391	110
5	2013–2016	12	-427	-390	60
6	2017–2020	13.5	-432	-390	80

Table S5. Reconstructed and predicted volumes of brine leaked from the evaporation ponds through different routes at each time period (in accordance with Figure 12 in the main text). Colors match those in Figure 12 in the main text.

mcm/year	1981–1990	1991–2000	2001–2008	2009–2012	2013–2016	2017–2020	2021–2030	2031–2040
Overall	**20**	**35**	**50**	**110**	**60**	**80**	**100**	**125**
The marine canal	10	18	25	35	39	55	70	87
Through Ye'elim fan	2	3.5	5.5	6.6	14.7	17	20.3	25.2
Beneath embankment northward	0	0.1	0.2	0.4	5	6	7.1	8.9
Through embankment northward	3	7	11.4	13.5	0.1	0.2	0.2	0.2
Through embankment eastward	5	6.4	7.9	54.5	1.2	1.8	2.4	3.7